

Tube Radial Distribution Flow Separation in a Microchannel Using an Ionic Liquid Aqueous Two-Phase System Based on Phase Separation Multi-Phase Flow

Kosuke NAGATANI,* Yoshinori SHIHATA,* Takahiro MATSUSHITA,* and Kazuhiko TSUKAGOSHI*.*†

*Department of Chemical Engineering and Materials Science, Faculty of Science and Engineering,
Doshisha University, Kyotanabe, Kyoto 610-0321, Japan

**Tube Radial Distribution Phenomenon Research Center, Kyotanabe, Kyoto 610-0321, Japan

Ionic liquid aqueous two-phase systems were delivered into a capillary tube to achieve tube radial distribution flow (TRDF) or annular flow in a microspace. The phase diagram, viscosity of the phases, and TRDF image of the 1-butyl-3-methylimidazolium chloride and NaOH system were examined. The TRDF was formed with inner ionic liquid-rich and outer ionic liquid-poor phases in the capillary tube. The phase configuration was explained using the viscous dissipation principle. We also examined the distribution of rhodamine B in a three-branched microchannel on a microchip with ionic liquid aqueous two-phase systems for the first time.

Keywords Ionic liquid aqueous two-phase system, phase separation multi-phase flow, tube radial distribution flow

(Received July 27, 2016; Accepted October 17, 2016; Published December 10, 2016)

Introduction

Two-phase separation mixed solutions, such as ionic liquid aqueous two-phase systems, separate into upper and lower phases through phase transformation in response to temperature change in a batch vessel.¹⁻⁵ On the other hand, when the same system is delivered into the microspace of a capillary tube or microchannel in a microchip under laminar flow conditions, a kinetic liquid-liquid interface is generated through phase transformation, leading to multi-phase flow.⁶⁻⁹ This specific type of microfluidic flow is called “phase separation multi-phase flow”, which is different from the conventional multi-phase flow (known as “immiscible multi-phase flow”) that occurs in mixed solutions composed of water and hydrophobic organic solvents. Phase separation multi-phase flow is observed with various two-phase separation mixed solvent systems, such as hydrophilic/hydrophobic organic ternary mixed solvents, aqueous surfactant mixed solutions, fluorocarbon/hydrocarbon organic mixed solvents, and aqueous ionic liquid mixed solutions (ionic liquid aqueous two-phase systems).^{7,8} Phase separation multi-phase flow occurs in many forms, such as droplets, slugs, parallel, and annular flow. Annular flow with inner and outer phases is observed under certain conditions, which is known as the “tube radial distribution phenomenon” (TRDP); the flow is termed as “tube radial distribution flow” (TRDF).⁶⁻⁹

Since the last century, phase separation or phase transformation in ionic liquid aqueous two-phase systems has been well known in the fields of analytical chemistry and separation science.^{1,10-13}

Ionic liquid aqueous systems separate into two distinct phases, namely an ionic liquid-rich phase and ionic liquid-poor phase, when cooled below a certain temperature.¹³ In our previous study,^{8,14} the TRDP and TRDF behavior of ionic liquid aqueous two-phase systems (*e.g.*, water-1-butyl-3-methylimidazolium chloride ([C₄mim]Cl)-KOH, water-[C₄mim]Cl-K₂HPO₄, and water-1-ethyl-3-methylimidazolium methylphosphonate ([C₂mim]MP)-K₂HPO₄) showing phase separation characteristics were examined by feeding into a capillary tube. However, there has been no information on the distribution behavior of a solute in the TRDF with ionic liquid aqueous two-phase systems. In this study we tried to examine the distribution of a solute in a microchannel on a microchip with ionic liquid aqueous two-phase systems for the first time.

Experimental

Reagents and capillary tubes

Water was purified with an Elix 3 UV water purification system (Millipore Co., Billerica, MA). All of the reagents used were purchased from commercial vendors and were of analytical grade. KOH, NaOH, and K₂HPO₄ were purchased from Nacalai Tesque, Inc. (Kyoto, Japan), whereas [C₄mim]Cl and [C₂mim]MP were purchased from Tokyo Chemical Industry Co. Ltd. (Tokyo, Japan). Rhodamine B was purchased from Wako Pure Chemical Industries (Osaka, Japan), and fused silica capillary tubes (inner diameter: 75 μm) were purchased from GL Science (Tokyo, Japan).

Bright-field microscope setup with a CCD camera system^{8,15}

A bright-field microscope-CCD camera system was set up to examine the capillary tubes (Supporting Information, Fig. S1).

† To whom correspondence should be addressed.
E-mail: ktsukago@mail.doshisha.ac.jp

A mixed solution containing rhodamine B was delivered into the capillary tube at a specific flow rate using a microsyringe pump, and was imaged using a bright-field microscope and CCD camera.

Microchip device^{16,17}

Figure 1 shows an enlarged view of a microchip containing triple-branched microchannels. A single wide channel (300 μm wide \times 40 μm deep), denoted as channel W, was separated into three narrow channels (100 μm wide \times 40 μm deep each), which were designated as channels N1 – N3. The microchip was set up to a microchip holder (Supporting Information, Fig. S2) for observation by a bright-field microscope with a CCD camera.

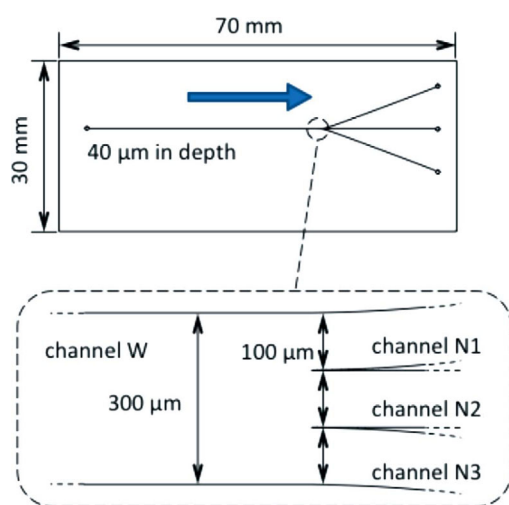


Fig. 1 Schematic representation of the microchip and enlarged view of the microchip containing triple-branched microchannels.

Results and Discussion

Fundamental experiments for TRDF

In our previous study, we examined the phase diagrams, viscosities, and TRDF images for three types of ionic liquid/water mixed solutions, namely water-[C_4mim]Cl-KOH, water-[C_4mim]Cl- K_2HPO_4 , and water-[C_2mim]MP- K_2HPO_4 systems.^{8,14} In the present study, the phase diagram, viscosity, and TRDF image of the water-[C_4mim]Cl-NaOH system was additionally examined. Figure 2 shows the phase diagram for this system, including solubility curves at 15 and 20 $^\circ\text{C}$. Transformation from the homogeneous to heterogeneous phases occurred upon changing the temperature from a high to low value. The volume ratios of the upper (ionic liquid-rich) and lower (ionic liquid-poor or aqueous) phases in a batch vessel are also presented in Fig. 2. The NaOH system was checked and considered regarding the following things, compared to the KOH system: 1) the appearance of salt precipitation in a batch vessel, as the KOH system showed precipitation at high concentrations of ionic liquid,¹⁴ and 2) the effect of the difference in the hydration behavior between hydrophobic ion (K^+) and hydrophilic ion (Na^+) on the phase diagrams. As a result, we could not observe salt precipitation in the experimental area for the NaOH system, and there was little difference in the solubility curve position on the phase diagrams between the systems.

The viscosities of the upper and lower solutions in the batch vessel were next examined at a room temperature (*ca.* 20 $^\circ\text{C}$). The average viscosities of the upper phase (ionic liquid-rich solution) and the lower phase (ionic liquid-poor solution) at five different compositions were 5.1 and 4.2 mPa·s, respectively (Supporting Information Fig. S3). The upper phase exhibited a higher viscosity compared to the lower phase, with a difference of about 1 mPa·s between the averages of the five compositions. Figure 3 shows TRDF images observed with a bright field microscope-CCD camera at a liquid flow rate of 1.0 $\mu\text{L min}^{-1}$. Regardless of the composition, the ionic liquid-rich solution

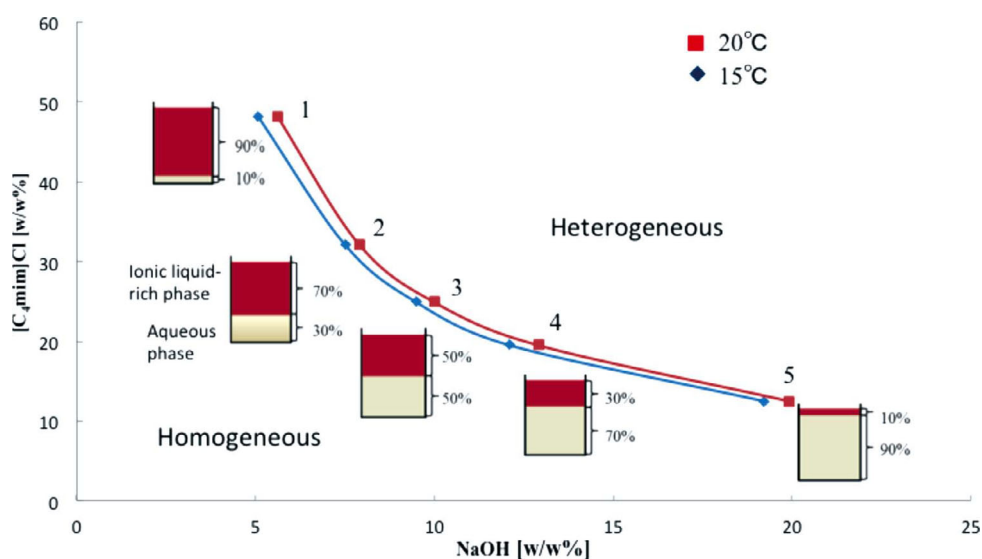


Fig. 2 Phase diagram of an ionic liquid/water mixed solution consisting of [C_4mim]Cl and NaOH at 15 (\diamond) and 20 $^\circ\text{C}$ (\square). The compositions of the homogeneous solutions (20 $^\circ\text{C}$), Nos. 1 – 5, represented by the symbols (\square) are as follows: (No. 1) [C_4mim]Cl:NaOH, 48:6 w/w %; (No. 2) 32:8; (No. 3) 25:10; (No. 4) 20:13; (No. 5) 13:20. Phase separation in a batch vessel at 15 $^\circ\text{C}$ is also illustrated for Nos. 1 – 5 with the volume ratios of the upper and lower phases, where the upper phase is ionic liquid-rich and lower phase is ionic liquid-poor (aqueous) phase.

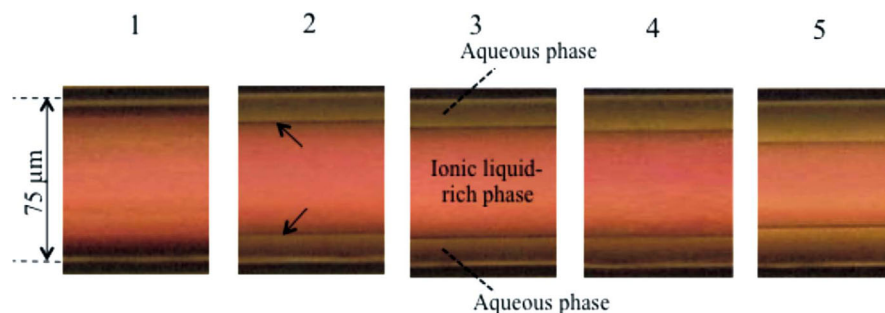


Fig. 3 TRDF image obtained with a bright-field microscope-CCD camera system of an ionic liquid/water mixed solution consisting of $[\text{C}_4\text{mim}]\text{Cl}$ and NaOH . Composition numbers 1 - 5 correspond to the definitions in Fig. 2. The arrows indicate the interface between the ionic liquid-rich and ionic liquid-poor (aqueous) phases. Conditions: Capillary tube, 120 cm length (effective length: 100 cm) and $75\ \mu\text{m}$ i.d. fused-silica; rhodamine B concentration, 5 mM; tube temperature, 15°C ; flow rate, $1.0\ \mu\text{L}\ \text{min}^{-1}$.

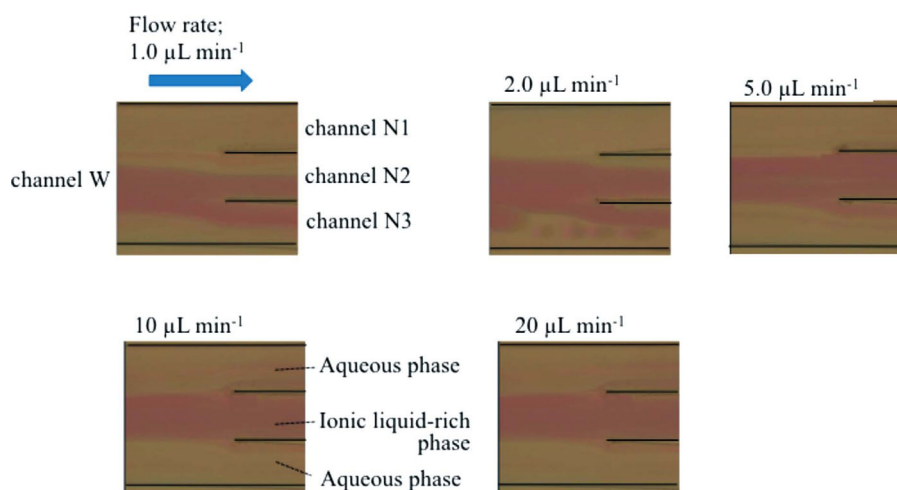


Fig. 4 TRDF images obtained with a bright-field microscope-CCD camera system of an ionic liquid/water mixed solution consisting of $[\text{C}_4\text{mim}]\text{Cl}$ and NaOH at 15°C in the triple-branched microchannels. Conditions: solution composition, $[\text{C}_4\text{mim}]\text{Cl}/\text{NaOH}$, 20:13 w/w%; rhodamine B concentration, 2 mM; temperature, 15°C ; flow rate, $1.0 - 20\ \mu\text{L}\ \text{min}^{-1}$.

flowed as the inner phase, whereas the ionic liquid-poor solution (aqueous solution) flowed as the outer phase. The TRDF for the solution with composition No. 5 seemed to be unstable; that is, the liquid-liquid interface tended not to stay at the same position, perhaps because of the construction with an inner phase having a rather small volume. The inner and outer phases were formed at various flow rates in the $1.0 - 20\ \mu\text{L}\ \text{min}^{-1}$ range.

In our previous paper, we discussed the configuration of the inner and outer phases in the TRDF from the viewpoint of the viscous dissipation principle and linear stability analysis.⁸ When there is a viscosity difference of over $0.7\ \text{mPa}\cdot\text{s}$ between the two phases, the phase with the higher viscosity forms the inner phase and the phase with the lower viscosity forms the outer phase, like water- $[\text{C}_4\text{mim}]\text{Cl}$ -KOH and water- $[\text{C}_2\text{mim}]\text{MP}-\text{K}_2\text{HPO}_4$.^{8,14} The configuration pattern was confirmed based on the viscous dissipation principle. On the other hand, when there was a viscosity difference of less than $0.7\ \text{mPa}\cdot\text{s}$ between the two phases, the larger volume phase formed an inner phase; that is, the phase configuration depended on the volume ratios, like water- $[\text{C}_4\text{mim}]\text{Cl}-\text{K}_2\text{HPO}_4$. The configuration pattern was explained based on the results of the linear stability analysis.^{8,18}

The configuration of the inner and outer phase in the water-

$[\text{C}_4\text{mim}]\text{Cl}-\text{NaOH}$ system, which of the viscosity difference was over $0.7\ \text{mPa}\cdot\text{s}$, was consistent with the experimental rule mentioned above, and followed the viscous dissipation principle. We must continue examining the availability of the rule hereafter through one-by-one experiments.

Distribution of rhodamine B based on TRDF in triple-branched microchannels

The ionic liquid research field is one of the most interesting and attractive.^{1,10-13} Also, many new types of ionic liquid are now being synthesized and reported, and their applications are widely investigated. The microfluidic behavior of the TRDF with the ionic liquid/water mixed solution was for the first time examined in microchannels in microchips, although the cross-sections of the channels were not of round shape, as described in the experimental section. The ionic liquid/water mixed solution (water- $[\text{C}_4\text{mim}]\text{Cl}-\text{NaOH}$; $[\text{C}_4\text{mim}]\text{Cl}$ 20 wt% and NaOH 13 wt%; the volume ration of upper and lower phases, 3:7 as shown in Fig. 2) containing 2 mM rhodamine B was fed into the microchannel of channel W on the microchip at a flow rate of $1.0 - 20\ \mu\text{L}\ \text{min}^{-1}$. Typical TRDF images in the triple-branched microchannels are shown in Fig. 4. The rhodamine B

molecule (red) is distributed near the center of channel W away from the inner walls of the channel. The rhodamine B molecule mostly appears to flow through the center channel (channel N2), whereas it is only slightly distributed in channels N1 and N3. Further, a stable distribution of rhodamine B in the center N2 channel was observed at higher flow rates of 10 and 20 $\mu\text{L min}^{-1}$, similarly to those described in the previous paper.¹⁶

Next, a homogenous ionic liquid/water mixed solution (water-[C₄mim]Cl-NaOH; [C₄mim]Cl 20 wt% and NaOH 13 wt%) containing 2 mM rhodamine B was fed into channel W at a flow rate of 20 $\mu\text{L min}^{-1}$. The solutions (100 μL) in channels N1 - N3 were collected through PTFE tubes into the corresponding vessels and subjected to absorption spectroscopy at 517 nm. The concentration of rhodamine B in the center channel (channel N2) and two side channels (channels N1 and N3) were 0.38 ± 0.03 , 2.60 ± 0.06 , and 0.40 ± 0.03 mM (they were average for five measurements), respectively. In other words, rhodamine B was distributed in the ionic liquid-rich phase in the central narrow channel rather than in the aqueous phases in the side narrow channels. The distribution pattern of the rhodamine B fluorescent dye in the triple-branched microchannels suggests that the TRDF in the channels could possibly be utilized for the extraction or separation of certain solutes.

Conclusions

We have examined the phase diagram, viscosity of the phases, and TRDF images for water-[C₄mim]Cl-NaOH mixed solutions. TRDF was observed with an inner ionic liquid-rich phase and outer ionic-liquid poor phase in the capillary tube. In addition, the distribution behavior of rhodamine B in a three-branched microchannel with TRDF using a water-[C₄mim]Cl-NaOH mixed solution was also examined. Although the results obtained are still fragmented, they constitute useful information for understanding TRDF and its application to various ionic liquid aqueous mixed solutions.

Acknowledgements

This work was supported by a Grant-in-Aid for Scientific Research (C) from the Ministry of Education, Culture, Sports, Science, and Technology, Japan (MEXT) (No. 26410165).

Supporting Information

Figures S1 - S3 are available free of charge on the Web at <http://www.jsac.or.jp/analsci/>.

References

1. K. E. Gutowski, G. A. Broker, H. D. Willauer, J. G. Huddleston, R. P. Swatloski, J. D. Holbrey, and R. D. Rogers, *J. Am. Chem. Soc.*, **2003**, *125*, 6632.
2. T. I. Horváth and J. Rábai, *Science*, **1994**, *266*, 72.
3. G. Tubio, B. Nerli, and G. Pico, *J. Chromatogr. B*, **2004**, *799*, 293.
4. H. Watanabe and H. Tanaka, *Talanta*, **1978**, *52*, 585.
5. N. Takahashi, M. Hashimoto, and K. Tsukagoshi, *Anal. Sci.*, **2013**, *29*, 665.
6. K. Tsukagoshi, *Anal. Sci.*, **2014**, *30*, 65.
7. K. Tsukagoshi, *J. Flow Inject. Anal.*, **2015**, *32*, 89.
8. S. Fujinaga, M. Hashimoto, K. Tsukagoshi, and J. Mizushima, *Anal. Sci.*, **2016**, *32*, 455.
9. M. Murakami, N. Jinno, M. Hashimoto, and K. Tsukagoshi, *Anal. Sci.*, **2011**, *27*, 793.
10. Y. Lu, W. Lu, W. Wang, Q. Guo, and Y. Yang, *Talanta*, **2011**, *85*, 1621.
11. C. Wua, J. Wanga, H. Wanga, Y. Peia, and Z. Li, *J. Chromatogr. A*, **2011**, *1218*, 8587.
12. Z. Li, Y. Pei, H. Wang, J. Fan, and J. Wang, *Trends Anal. Chem.*, **2010**, *29*, 1336.
13. J. Han, Y. Wang, Y. Li, C. Yu, and Y. Yan, *J. Chem. Eng. Data*, **2011**, *56*, 3679.
14. S. Fujinaga, K. Unesaki, K. Kitaguchi, Y. Kawai, K. Nagatani, M. Hashimoto, K. Tsukagoshi, and J. Mizushima, *Anal. Sci.*, **2014**, *30*, 1005.
15. T. Kobayashi, H. Kan, K. Tabata, M. Hashimoto, and K. Tsukagoshi, *J. Liq. Chromatogr. Relat. Technol.*, **2015**, *38*, 44.
16. N. Jinno, M. Hashimoto, and K. Tsukagoshi, *J. Anal. Sci., Meth. Instrum.*, **2012**, *2*, 49.
17. N. Suzuki, M. Hashimoto, and K. Tsukagoshi, *Solvent Extr. Res. Dev., Jpn.*, **2016**, *23*, 115.
18. D. D. Joseph, Y. Renardy, and M. Renardy, *J. Fluid Mech.*, **1984**, *141*, 309.